TRANSGRANULAR FRACTURES IN THE DAMAGE ZONE OF THE PUNCHBOWL FAULT

An Undergraduate Research Scholars Thesis

By

MELISSA ZAMBRANO

Submitted to Honors and Undergraduate Research
Texas A&M University
In partial fulfillment of the requirements of the designation as

UNDERGRADUATE RESEARCH SCHOLAR

Approved by
Research Advisor: Dr. Judith Chester

May 2013

Major: Geology

TABLE OF CONTENTS

ABSTRACT

Transgranular and Intragranular Fractures. (May 2013)

Melissa Zambrano
Department of
Geology
Texas A&M University

Research Advisor: Dr. Judith Chester
Department of
Geology and Geophysics

Understanding faults is challenging but not impossible. Looking at the Punchbowl fault, an ancient trace of the San Andreas Fault in the Transverse Ranges of southern California, is one way to understand a fault that has been studied for years and still hasn't been fully understood. I am interested in grasping the formation and structures of the damage zone of large displacement continental transform faults, in particular the San Andreas Fault. To do this, I characterized the fractures in the damage zone of the Punchbowl Fault. The fractures associated with the Punchbowl Fault include open mode fractures, transgranular cracks, transgranular filled cracks, calcite filled veins, hematite filled veins, shear fractures, and the list continues. The Punchbowl formation rock samples had already been gathered by other students and I went back and looked at new traits of the fracture system, specifically on the microscale. I separated the fractures into three categories; open fractures (OF), shear fractures (SF), and shear fractures with fill (SOF). Each of these rock samples were put on thin sections to observe on a microscale. Eventually I was able to count the number of fractures on a coarse grid and determine the fracture density. The fracture density data showed a decrease in fracture density the further away the samples

were located. The primary focus was mainly on the shear fractures and open mode fractures these were the largest fractures in the thin sections. I focused on these to make sure that the fracture densities would follow those of other ancient traces of the SAF. I found that the damage zone of the San Gabriel Fault [Becker, 2012] and the San Andreas Fault at the San Andreas Fault Observatory at Depth [Ayyildiz, 2012] both matched the fracture density assortment I found for the Punchbowl fault.

DEDICATION

To my Mother, who has always been a constant

source of encouragement and support

AWKNOWLEDGEMENTS

I would like to thank my advisor in this endeavor, Dr. Judith Chester, for giving me a chance as her student and patiently guiding me through the process. Also I would like to say thank you for teaching me so much throughout this year.

Another thank you to Alpherd Wright for helping me with thin sections. I would also like to thank Daniel Elizondo-Ugarte for helping me throughout the process.

Finally I would like to thank my Mother for her encouragement. And to all my friends who let me vent to them, especially Abigail Baden-Robinson and Jason Miller.

NOMENCLATURE

SAFOD	San Andreas Fault Observatory Depth
SAF	San Andreas Fault
PBF	Punchbowl Fault
SGF	San Gabriel Fault
OF	Open Fracture
SOF	Shear Fractures with Fill
SF	Shear Fractures

CHAPTER I

INTRODUCTION

There have recently been a number of devastating earthquakes reinforcing the need for a better understanding of active faults (Figure 4). By comparing the Punchbowl Fault, an ancient trace of the San Andreas Fault (SAF), to the active trace of San Andreas System, we can gather data to predict future actions of the SAF. Drilling into an active fault is one way to get a better understanding of the processes of earthquake generation. Through such drilling, rock samples are retrieved from the earthquake-generating portion of a fault (e.g., 2 to 20 km depth in a continental transform fault) so they can be studied in detail in the laboratory [e.g., Zoback et al., 2010]. My work will be compared to data gathered from core taken along that active fault to better understand the system.

The SAF system began developing about 30 million years ago (Figure 3). At this time the Pacific Plate contacted the North American Plate along the California continental borderland. Before this, the Farallon Plate was subducting under the North America. The Juan de Fuca, Rivera, Cocos, and Nazca plates are considered discontinuous remnants of the Farallon Plate (Figure 3) [Chester, 1999]. The first significant trace of the southern portion of the SAF was the Clemens Well-Fenner-San Francisquito Fault zone (22-13 Ma). The San Gabriel Fault (SGF) became the primary strand of movement from 10 to 5 million years ago. After some time, movement shifted from the San Gabriel Fault switched to the Punchbowl Fault (5 to 1 Ma), and then to the current active trace in this region. [Dolan et al., 2007] hypothesize that eventually the Eastern California Shear Zone will take over movement around the Garlock Fault north of this area.

The Punchbowl Fault (PBF) is an ancient exhumed fault of the San Andreas system in southern California [Chester and Logan, 1986; Chester et al., 1993; Chester and Chester, 1998; Chester et al., 2004; Schulz and Evans, 1998, 2000; Wilson et al., 2003]. The Punchbowl Fault, and similar inactive exhumed faults [Chester et al. 1993], often are given as type examples for the structure of active faults at depth [Chester et al. 1993]. This view, however, comes with some uncertainty because inactive, exhumed faults can display chemical alteration and deformation overprinting associated with uplift and exhumation [Chester et al. 2004].

The Punchbowl Fault is best exposed in Devil's Punchbowl County Park, California (Figure 2). This fault is widely used as a model for the fault zone structure of the active, locked segments of the SAF Fault system at 2 to 4 km depth [Chester et al. 1993]. The Devil's Punchbowl Country Park area is of moderate relief between the San Gabriel Mountains and Mojave Desert. This area was eroded to low relief in Pleistocene time and covered by alluvial fans when the region was uplifted; erosion exposed Punchbowl Formation that is cut by the fault. In this study, I will use samples of the Punchbowl Formation, collected by J.S. Chester, for the fracture analysis.

The SAF is one of the most studied fault systems in the world. The SAF is a right-lateral continental transform fault that is approximately 1,300 km long [Zoback, 2010]. Through these studies scientists have learned a great deal about continental transform systems and the devastating earthquakes that occur along then. The objective of this study is to understand the deformation produced at seismogenic depths during displacement along this system. To do this, I will study the damage zone of the Punchbowl Fault, an exhumed inactive trace of the SAF system exposed northeast of Los Angeles, California. Specifically I will characterize the density distribution of transgranular fractures in the Punchbowl Formation adjacent to the Punchbowl

Fault trace. I want to determine if the transgranular fractures are similar to the mesoscale faults and microscale, Mode I-type fractures.

CHAPTER II

METHODS

Punchbowl Formation Samples

The Punchbowl Fault is an inactive, exhumed fault of the San Andreas transform system in the central Transverse Ranges of southern California (Fig. 1). The Punchbowl Fault is about 5 km southwest of the SAF. This fault has experienced approximately 40 km of right lateral motion. The Punchbowl Fault juxtaposes the Punchbowl Formation arkosic sandstone and igneous rocks in the region where the samples were collected. The Punchbowl Fault dips to the southwest and has a sinuous trace. The fault cuts the crystalline rock of the San Gabriel basement complex and in some places is covered by Paleocene Quaternary rock. The samples collected were cut into small blocks and polished to prepare thin sections for microscopic observation. Related work done on the samples is reported in Chester et al. [1993] and Wilson et al. [2003].

Microstructural characterization

When beginning the process of evaluating the Punchbowl Fault there were thin sections made from previous projects [e.g., Chester et al., 1993; Wilson et al., 2003]. For the microstructural characterization, one to three mutually perpendicular petrographic thin sections were made from the samples. These sections are defined by an outward normal to each thin section plane and are referenced to a cube (Figure 1). Plane- and cross-polarized light digital scans were taken of each thin section. These thin section scans were used as location maps for the fracture density measurements. Thin sections were used to collect thin section scale transgranular fracture density data, and intragranular scale fracture density data (Tables 1 and 2).

Microscale fracture density measurements

Using a mechanical stage on a petrographic microscope I collected linear transgranular fracture density (LIFD) data for the Punchbowl Fault. In addition, intragranular fracture density data were collected from quartz grains that were larger than 0.25cmm in diameter using a 3-mm square grid. I analyzed the different fractures throughout the thin section samples.

Transgranular fracture

The number of the transgranular fractures were measured from three mutually perpendicular petrographic thin sections, taken from the Punchbowl Fault area using a petrographic microscope following the methods described by Becker *(*2012). For non-planar transgranular fractures, I recorded the number of fractures crossing the 3-mm grid and noted the fracture type. The fracture types (open, sealed, and shear fractures) were recorded in an excel spreadsheet (Table 3), and mapped and numbered on the image scans using Adobe Illustrator. Using Adobe Illustrator, I mapped the location of each type of fractures in a unique layer.

Intragranular fractures

The number of intragranular microfractures was counted using a method modified from the way I collected transgranular fractures. Only Open Mode I-type fractures were counted. Grains that had a Mode-I fracture that cut entirely through the largest grains were counted as an intragranular fracture in the thin sections. These grains had to be approximately 0.25 mm in diameter. I was marked these fractures first on the paper copies with a sharpie and then mapped them in the Adobe Illustrator files. With the data from the three mutually perpendicular thin sections (Figure1) we could pick out the fractures needed to identify the intensity of the fractures present in the sample. Feldspar grains were used in quartz-poor samples, when necessary. Within each grain, the number of fractures intersecting a count line was recorded. The orientation of the line, length of the line, number of fracture intercepts, and fracture type (i.e., open, healed, sealed) were recorded. Mostly large quartz grains were used to record the intragranular fractures, as well as a few feldspar grains.

CHAPTER III
RESULTS

Description of The Punchbowl Formation samples

Rock type and grain size

All of the samples used for this study are arkosic sandstones. This is evident because the samples were located on the northeastern side of the fault (Figure 2). Also just by simply identifying the rock type one can see the samples were all arkosic sandstones. Figure 2 shows the actual locations of each of the samples. They were collected along mesoscale fracture density traverses lines of Wilson et al. [2003]. The mesoscale fracture density increases as the fault is approached [Wilson et al. 2003]. The samples located here ranged from coarse grained to fine grained sandstones. The finer grained samples were further away, approximately 10 km away from the Punchbowl Fault. The samples collected further away were more intact. For a list of samples used in this study is given in Table 2.

Cement type and extent of cement

There are a few types of cements found in Punchbowl Formation sandstones. The most common found in the samples collected were calcite, hematite, and laumonite [Wilson et. al. 2003]. Some of these samples have more than one type of cement. The closer the sample was to the main Punchbowl Fault, the greater the volume of cements. Clay is also present as a cement in these samples. For more detailed information on what samples were filled with what cement, refer to Table 1. When dealing with the extent of the cement in the thin sections, there tended to be a trend. The trends lead me to believe that the cement was mostly apparent when closest to the Punchbowl Fault. The closer the sample of rock, the more cement is present in the thin section (Figure 2) (Table 1).

Fracture characterization

Qualitative fracture density

During the collection of fracture density a 3mm-square grid was placed on the thin sections in Adobe Illustrator. I used this grid to count the fractures present in each of the thin sections analyzed. This made it possible to count how many fractures that were in a specific area crossed a specific grid line. At first it did not matter what kind of fracture was present in the given area as long as the fracture was counted up. This indicated a more specific number of fractures that were present in the smaller given area. Once the number of fractures were counted and added up to find the total of fractures given in one sample I calculated the density and made Table 3. The table has both the number of fractures found on the grid line and it also has the type of fracture found. I also made different tables with the exact grid line location versus the type of fracture found. These other tables were just used to find the density to a more specific level while Table 3 was an overview of all the fractures and their locations. I used the same Adobe Illustrator settings for each thin section.

Qualitative estimate of number of fracture

The number of fracture set orientations is based on the number of fractures that were found. During the creation of the fractures that were looked at further. I recognized that there were quite a few slides that showed a pattern with the fractures. The pattern appeared to be that the fracture density with distance to the Punchbowl Fault would be affected. It would be affected because of the sheerness of the Punchbowl Fault. The closer the location of the rock samples to the Punchbowl the higher the number of fractures occurred. It appears that throughout the samples that are closest to the Punchbowl Fault, by distance, are those samples with the most fractures and those fractures are predominantly filled with calcite of hematite.

Type of fractures present and fracture fill

There are 18 thin sections that were looked at in closer detail out of the 64 thin sections of the Punchbowl Formation that were initially surveyed and scanned. Out of these 18 thin sections, a number of different fracture types were noted. The thin sections chosen for this study had at least one additional, mutually perpendicular section from the same sample that was available for study (Table 3). Before working with Adobe Illustrator, I mapped all of the fractures on paper copies of the image scans printed for each thin section. Each fracture type was traced with a unique color (Table 4). Six different fracture types were identified in the in the Punchbowl Formation samples studied. Most fractures were transgranular fractures; one set of intragranular fractures were mapped because I deemed these were important for this study.

Transgranular fractures deal with open mode, calcite filled veins, and hematite filled veins, transgranular cracks, gouge zones, and shear fractures. Intragranular grains deal with open mode fractures, sealed either with calcite, hematite, or Laumonite, or healed of fluid inclusions (Table 4). There were three levels of thin section (high to low fractures present) by the end of the thin section analysis it was easy to distinguish if a fracture was more likely to have a shear fracture running through it or if it was more likely to have open mode to transgranular cracks only. The further away from the Punchbowl Fault the less shear fractures present.

Thin section arrangement

During the last two months, I have been looking at different samples located near the Punchbowl Fault (Figure 2). These rock samples have been placed on a thin section by cutting the rocks down with a diamond blade until it was the smallest possible and then was sand down with sand paper until the rock samples on the thin sections were small enough to be used on a microscope. Some of these samples have thin sections of the same rock but cut on mutually perpendicular sides giving us a better view of the fractures within. I than began scanning each thin section. There were approximately 64 thin sections to scan for the Punchbowl Fault. After scanning the thin sections I began the process of looking through the thin sections and organizing them based on how fractured they were. Of course, the most fractured samples were found nearest to the Punchbowl Fault. If you look at Table 2 you can see what traverse each thin section came from. By knowing what traverse location from Table 2 you can use that information and correlate it to the location map Figure 2.

Based on their locations the thin sections were then broken up into three different categories. The highest fractured set of thin section included the set of DP10_B, DP11_I, and P45. These thin sections had the highest density of fractures. With all three of these sets having a substantial amount of transgranular cracks (Table 5). The second set of thin sections are in the middle, they don't have a substantial amount of fractures but more than in the lowest set of thin sections. This set of thin sections only contain DP10_E. The group of thin section DP10_E was the only set of thin sections that only had two perpendicular sides instead of the three that the rest of the thin sections had in this project. These thin sections were relatively close to the Punchbowl Fault and had shear fractures with fill. The main difference between this set of thin sections and the first was that DP10_E was no longer shattered like the first sets of thin sections were. The last group has the lowest amount of fractures present in them. This includes P9 and P18. P9 was there furthest sample taken from the Punchbowl Fault, which indicates a correlation between distance and the amount of fractures present. However, P18 did show an oxymoron of information since in contrast from its distance to that of P9 there should have been a greater difference in fractures present. To see more detailed information on what fractures are found in what thin section see Table 5.

CHAPTER IV
CONCLUSIONS

4.1 Discussion

Now that we have differentiated the different fractures present in the area, and decided what fracture fell into what category, we are able to determine the fracture density (if enough fractures were present in the sample). Being able to determine this is what the entire project was about. I wanted to be able to determine that the Punchbowl Fault has similar characteristics to that of the SGF and SAF to determine the likelihood that the next large Earthquake could be slightly better predicted just based on how both the SGF and the Punchbowl Fault occurred in the past. Knowing the densities shows us the effectiveness of an earthquake to cause more fractures to occur in the rock.

4.2 Final Conclusion

Finally looking at our Table 3 we can clearly differentiate between the thin sections that had larger densities and those that have low densities. By looking at this table we clearly can see that the thin sections that we had originally put in our “high” estimated density thin sections are clearly the ones with the most intersections of grid lines. As such the trend continues to our “medium” and “low” density estimates as well. During the process of thin section analysis I did notice that there were thin sections that we could eliminate and therefore that is why there were only 18 thin sections that were looked further into. I also made sure that I could see the trend that had been proven in the other studies dealing with the SAF and SGF. Meaning, I wanted to see if the fracture density decreased the further away I went from the main fault.

REFERENCES

Almeida, R., (2007). Mesoscale Fracture Fabric and Paleostress Along the San Andreas Fault at SAFOD (Masters dissertation). Texas A&M University, College Station, TX.

Becker, A., (2012), Off-Fault Damage Associated With A Localized Bend in the North Branch San Gabriel Fault, California (Masters dissertation). Texas A&M University, College Station, TX.

Chester, F. M., J. P. Evans, and R. L. Biegel, Internal Structure and Weakening Mechanisms of the San Andreas Fault, *J. Geophys*. Res., 98, 771-786, 1993.

Chester, F. M., 1999. Field Guide to the Punchbowl Fault Zone at Devil's Punchbowl Los Angeles County Park, California, Center for Tectonophysics, (2.1).

Dolan, J. F.,Bowman, D. D., and Sammis, C. G. (2007). Long-range and long-term fault interactions in southern California, *Geology*. Vol. 35, pp. 855-858

Friedman, M., 1969. Structural Analysis of fractures from Saticoy Field, Ventura Country, California, *AAPG*, 53 (2), 367-389.

Laubach, S.E., Olson, J.E., and Gross, M.R., 2009. Mechanical and Fracture Stratigraphy, *AAPG Bulletin*, 93 (11), 1413-1426.

Hickman, S., Zoback, M., and Ellsworth, W., 1994. Deep Scientific Drilling in the San Andreas Fault Zone, *EOS Trans. AGU*, 75 (12), 137-144.

Hickman, S., Zoback, M., and Ellsworth, W., 2004. Introduction to special section: Preparing for the San Andreas Fault Observatory at Depth, *Geophysical Research Letters*, 31 (L1S12), 1-4.

Ramsey, J.M. and Chester, F.M., 2004. Hybrid Fracture and the Transition from Extension Fracture to Shear Fractures, *Nature*, (428), 63-66.

Roeloffs, E., 2000. The Parkfield, California Earthquake experiment: An update in 2000, *US Geological Survey*, 79 (9), 1226-1237.

Wallace, R.E., 1990. The San Andreas Fault System, California, *US Geological Survey Professional Paper*, Paper 1515.

Wilson, J. E., Chester, J. S., and Chester, F.M. 2003. Microfracture analysis of fault growth and wear processes, Punchbowl Fault, San Andreas system, California, *Journal of Structural Geology*, 25, 1855-1873.

Zoback, M., Hickman, S., and Ellsworth, W., 2010. Scientific Drilling Into the San Andreas Fault Zone, *EOS Trans. AGU, 91 (22)*, 197-199.

Zoback, M., Hickman, S., and Ellsworth, W., 2011. Scientific Drilling Into the San Andreas Fault Zone – An overview of SAFOD's first five years, *EOS Trans. AGU*, 14-28.

FIGURES:

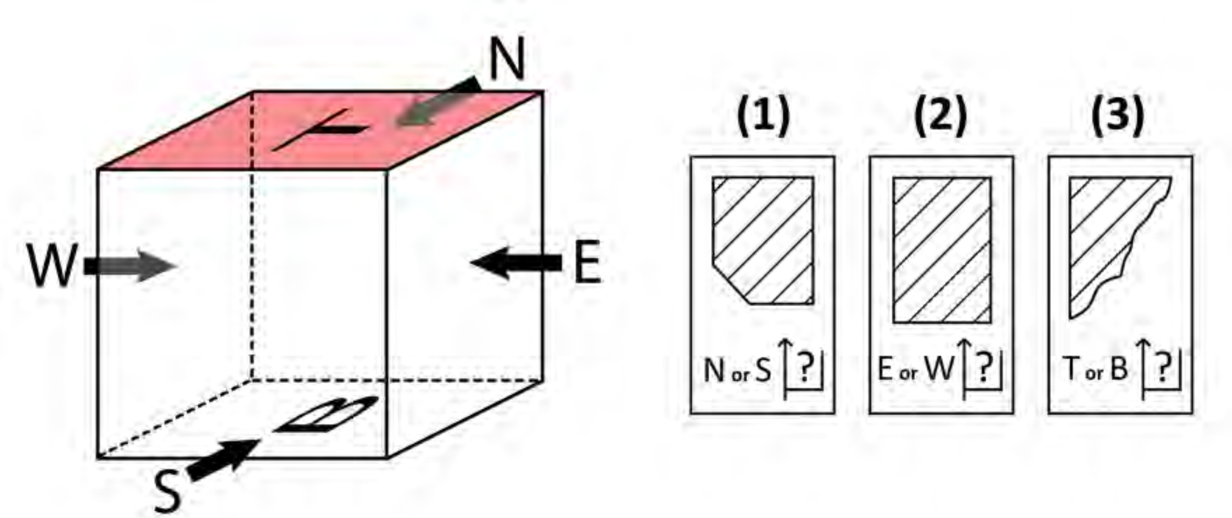

Figure 1**.** Oriented sample guide cube. Schematic diagram of the guide cube used to orient each sample. Three mutually perpendicular thin sections are cut from each sample: (1) north or south plane, (2) east or west plane, and (3) top or bottom plane [From Becker, 2012].

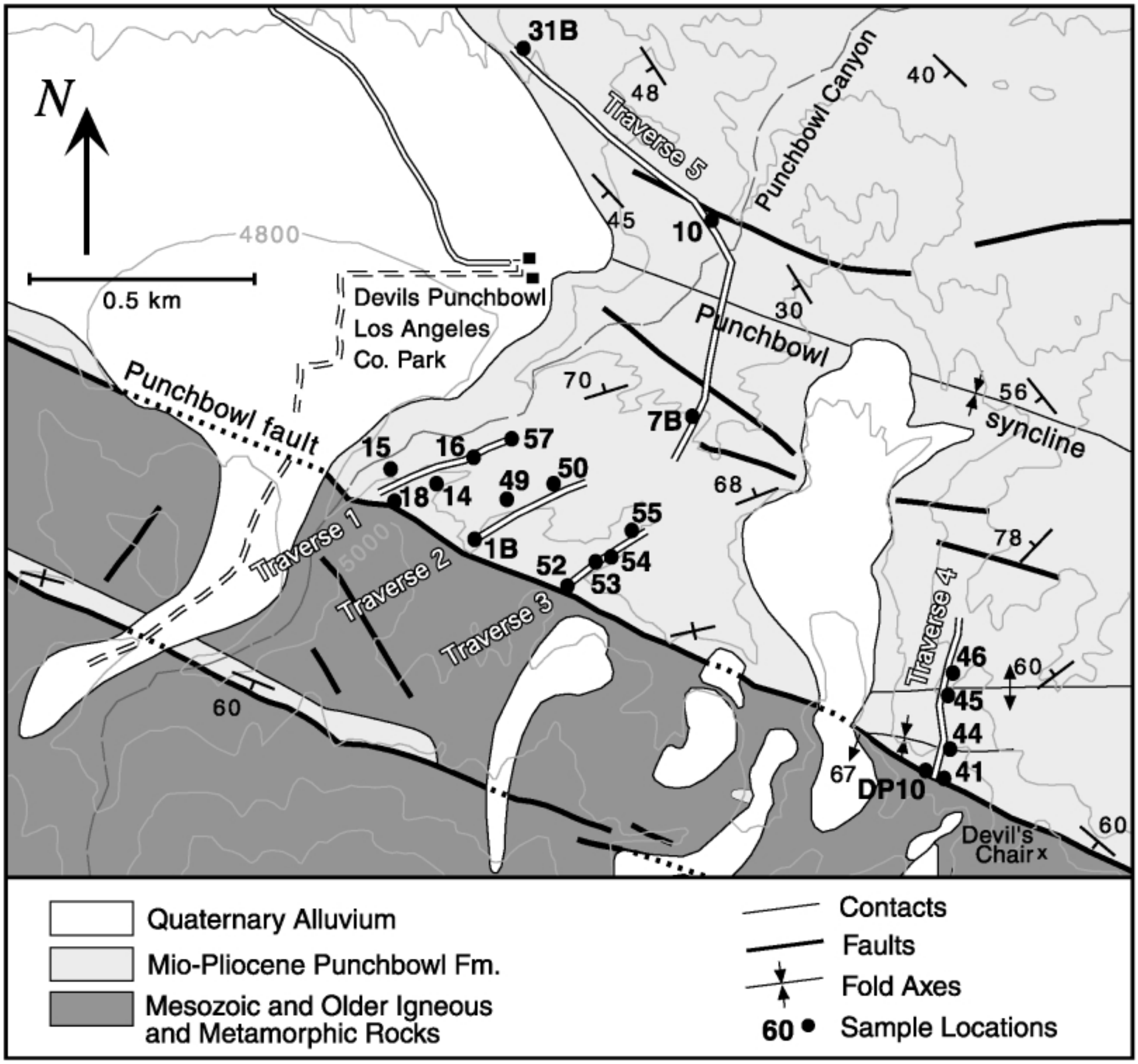

Figure 2. Geologic map of the Devil's Punchbowl showing the sampling locations along several traverses away from the Punchbowl fault and across axes of folds in the Punchbowl Formation. [From Wilson et al., 2003].

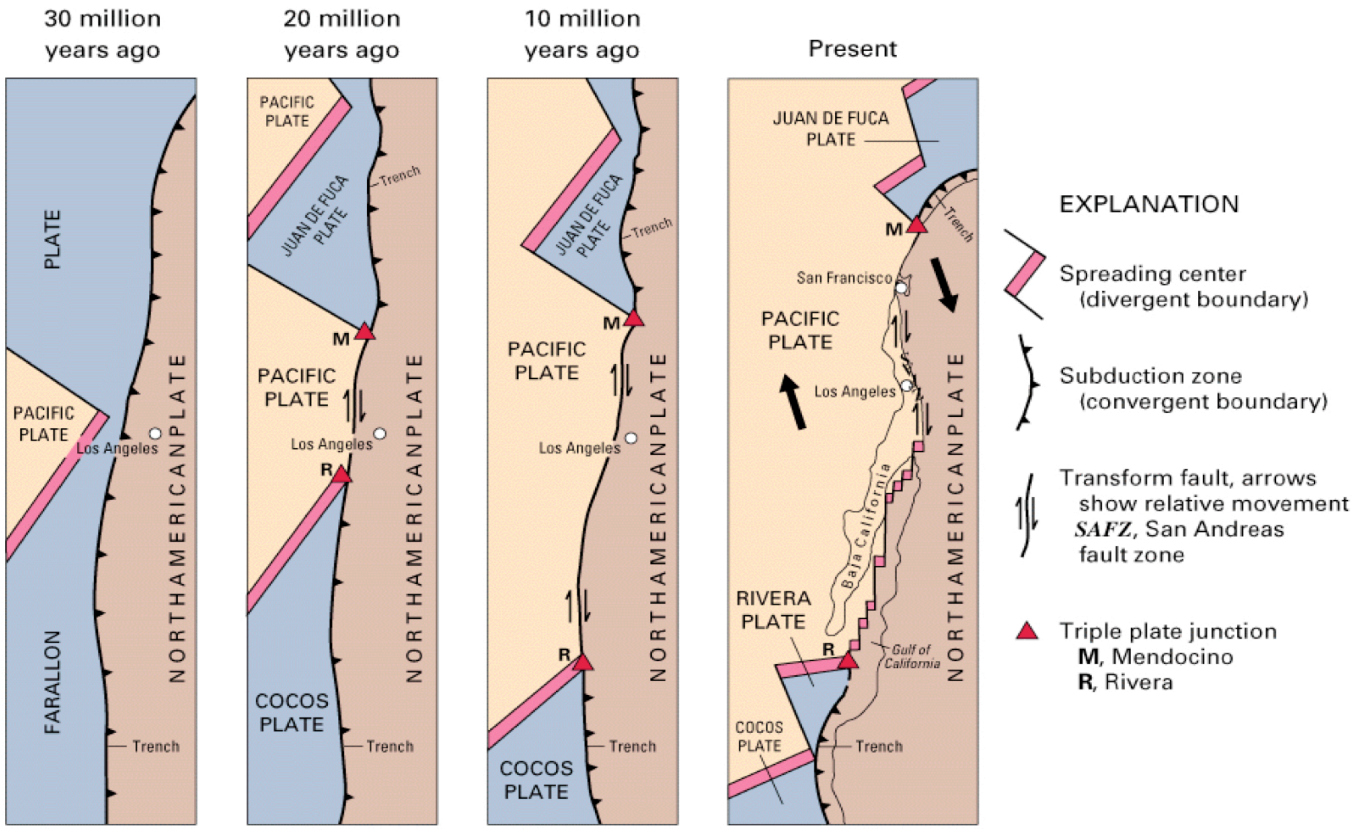

Figure 3. Schematic diagram showing the last 30 million years of evolution of the California continental margin. From USGS Professional Paper 1515

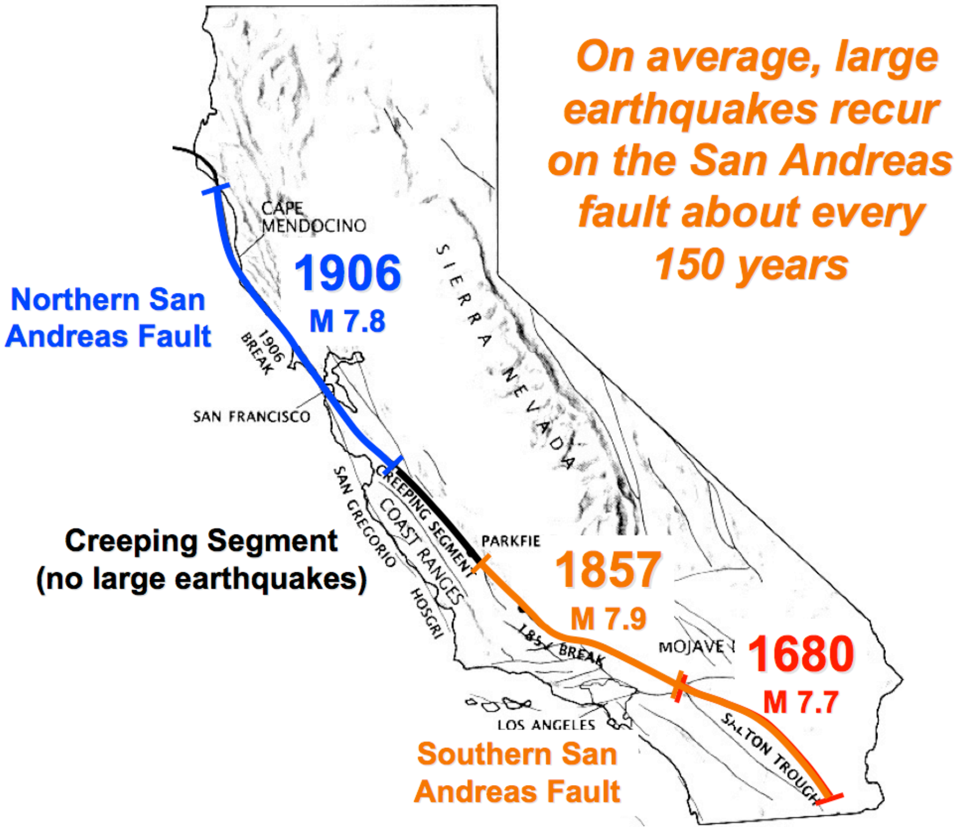

Figure 4. Earthquake Country Alliance, Putting Down Roots Publication produced by the Southern California Earthquake Center (SCEC) [From Wallace, 1990].

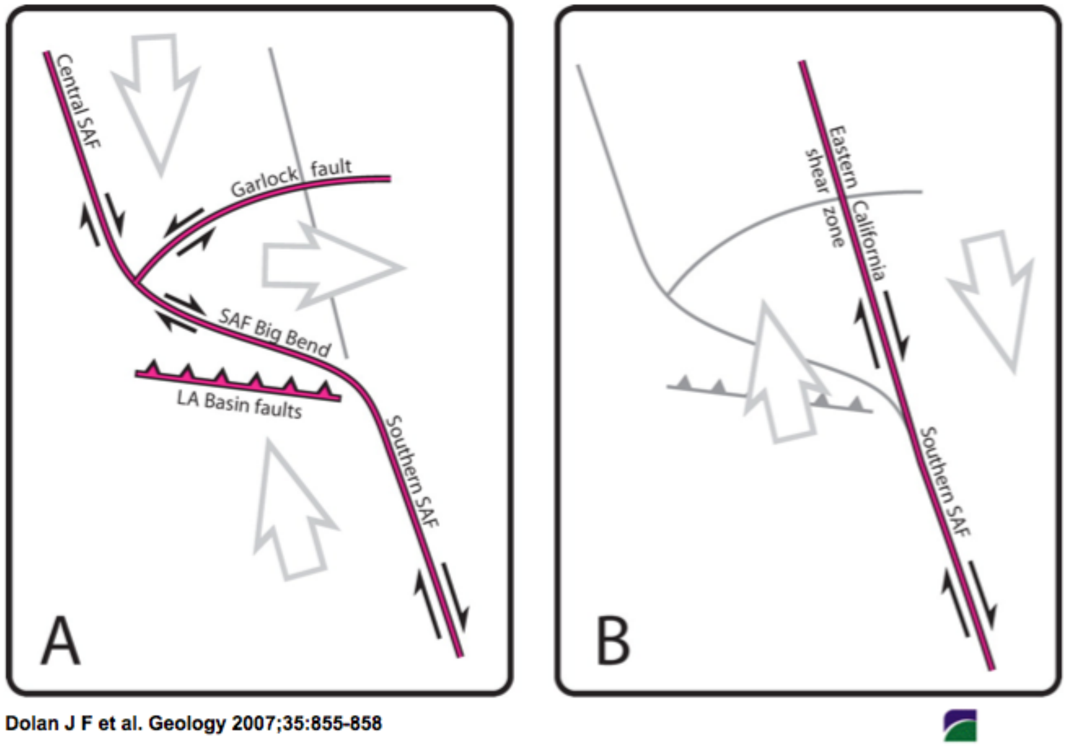

Figure 5. This shows the direction of the San Andreas Fault from the way it use to cut through California (A) to the way it has shifted to how it is now (B) [From Dolan, 2007].

TABLES:

Table 1. List of Samples and Thin Sections from the Punchbowl Formation [a]

Sample	Distance[c] (m)	Traverse	Rock Type	Cement Type	Cement Extent [b]	Fabric Domains[d]	Distance to Subsidiary Faults
DP10_B	0.075	4	Cataclastic ss			IDZ-FC	cm
DP10_E							
P18	12	1	Medium ss	Laumonite And Clay	Moderate	MDZ, ODZ	10s m
DP11_I	14.2	4	Medium-coarse ss			MDZ	cm
P45	200	4		Calcite	Extensive		
P9	780	Fold Test Traverse		Laumonite			
DP13_A							

[a] Table was modified from Wilson et al. (2003) and Wilson (1999)
[b] Moderate = ~5%; extensive = ~20%; very extensive = ~30%
[c] Distance from ultracataclasite layer.
[d] IDZ-FC = innermost damage zone and fault core; MDZ = middle portion of damage zone; ODZ= outer damage zone; PS = five samples across Punchbowl syncline

Table 2. List of Thin Sections Taken from Samples of the Punchbowl Formation[a]

Sample	Thin Section	Distance [b] (m)
DP10_B	DP10_B-2	0.075
	DP10_B_B-2	0.075
	DP10_B_1-B	0.075
	DP10_B_2-B	0.075
DP10_E	DP10_E_4-1	
	DP10_E_2-T	
P18	P18_S-W	12
	P18_T-S	12
	P18_W-N	12
DP11_I	DP11_I_B-4	14.2
	DP11_I_2-T	14.2
	DP11_I_2-B	14.2
	DP11_I_3-4	14.2
P45	P45_W-N	200
	P45_T-N	200
	P45_S-E	200
P9_N	P9_N-B	780
	P9_T-N	780
	P9_W-S	780

[a] Table was modified from Wilson et al. (2003) and Wilson (1999)
[b]Distance from ultracataclasite layer

Table 3. Transgranular Fracture Density Determined from Whole Thin Section Mapping (3mm Grid.)

Thin Section	Total Vertical Grid Line (mm)	Total Horizontal Grid Line (mm)	Total Overall Grid Length (mm)	Total # of Fractures with Vertical Lines	Total # of Fractures with Horizontal Lines	Total # of Fractures
DP10_B_2-T	189	210	399	98	62	160
DP10_B_B-2	87	99	186	42	27	69
DP10_B_1-B	186	186	372	53	93	146
DP10_B_2-B	225	234	459	74	93	167
DP10_E_2-T	225	237	462	41	48	89
DP10_E_4-1	222	255	477	32	16	48
DP11_I_2-B	183	168	351	28	29	57
DP11_I_2-T	114	126	240	4	16	20
DP11_I_3-4	192	198	390	35	21	56
DP11_I_B-4	195	186	381	17	22	39
P9_N-B	159	171	330	9	10	19
P9_T-N	210	240	450	3	2	5
P9_W-S	192	219	411	0	2	2
P18_S-W	231	240	471	15	9	24
P18_T-S	180	180	360	16	24	40
P18_W-N	231	237	468	31	48	79
P45_W-N	189	189	378	35	21	56
P45_T-N	210	189	399	16	20	36
P45_S-E	210	189	399	41	28	69

Table 4. List of Fractures found in Thin Sections with Corresponding Colors [a]

Type of Fracture	Abbreviation	Color
Open Mode	OF	Purple
Calcite Filled	SOF	Pink
Hematite Filled	SOF	Lime Green
Transgranular Crack	TG_M1	Red
TG Sheared-Calcite, Hem, Laumonite	SF	Cyan
Intragranular	OF	Orange
TG Sheared without Gouge	SF	Yellow

[a] This was the color coding for Adobe illustrator and hand traced

Table 5. List of Thin Sections with the Fractures Found in Each

Thin Section	Open Mode	$CaCO_3$ Fill[a]	Fe Fill [b]	Trans Crack	Intragran[c]	Trans Fill	Shear	G-Zone[d]
DP10_B-2	Y	Y	Y	Y	N	N	N	N
DP10_B_B-2	Y	Y	Y	Y	N	N	N	N
DP10_B_1-B	Y	Y	Y	Y	N	N	N	N
DP10_B_2-B	Y	Y	Y	Y	N	N	N	N
DP10_E_4-1	Y	N	Y	Y	N	N	N	N
DP10_E_2-T	Y	N	Y	Y	N	N	N	N
P18_S-W	N	N	N	Y	N	N	Y	N
P18_T-S	Y	N	N	Y	N	Y	N	N
P18_W-N	Y	N	N	Y	N	N	Y	N
DP11_I_2-T	Y	N	Y	Y	N	N	Y	N
DP11_I_B-4	Y	N	Y	Y	N	N	Y	N
DP11_I_2-B	Y	N	Y	Y	N	N	Y	N
DP11_I_3-4	Y	N	Y	Y	N	N	Y	N
P45_W-N	N	Y	N	Y	Y	N	N	N
P45_T-N	N	Y	N	Y	Y	N	N	N
P45_S-E	N	Y	Y	Y	Y	N	Y	Y
P9_N-B	N	N	Y	Y	N	N	Y	N
P9_T-N	N	N	Y	Y	N	N	Y	N
P9_W-S	N	N	Y	Y	N	N	Y	N

[a] Calcite filled veins
[b] Hematite filled veins
[c] Intragranular fracture
[d] Gouge Zone
Y= yes they are present
N= No they are not present